Estimation of whistling of an orifice in a reverberating duct at low Mach number

Romain Lacombe, Pierre Moussou, Yves Aurégan

ACOUSTICS 2012

Estimation of whistling of an orifice in a reverberating duct at low Mach number

R. Lacombe[a], P. Moussou[a] and Y. Aurégan[b]

[a]EDF R&D, 1, avenue du Général de Gaulle, 92241 Clamart Cedex, France
[b]Laboratoire d'acoustique de l'université du Maine, Bât. IAM - UFR Sciences Avenue Olivier Messiaen 72085 Le Mans Cedex 9
romain.lacombe@edf.fr

Single hole circular orifices can generate pure tone noise in industrial pipes. This phenomenon results from vortex shedding with lock-in, as a consequence of an acoustic amplification of incipient pressure waves inside the orifice and of an acoustic resonator outside. Key features of this phenomenon are the ability of an orifice to amplify acoustic waves in a range of frequencies and the acoustic feedback mechanism. First, the study deals with the estimation of the whistling ability of an orifice from an incompressible flow simulation. As the studied flow is limited to low Mach number, this kind of simulation fairly describes the hydrodynamic instability. Superimposed harmonic velocity perturbations allow then to identify the impedance of an orifice and so to define the frequency at which amplification occur. The next step of the study deals with whistling features of orifices in a reverberating duct. The extracted impedance is used in a network model, taking into account acoustic propagation and acoustic reflections. A linear stability analysis is then performed and the whistling frequency is predicted. The parameters controlling the whistling amplitude are finally identified. All the results of the study are compared to experiments, showing well agreements for the whole procedure.

1 Introduction

Orifices in confined duct submitted to flow are known to generate pure tones [1, 2, 3, 4]. These tones comes from the combined effects of self-sustained oscillations and of non-linear saturation mechanisms. Along the shear layer surrounding the jet created when the flow past the orifice, the interaction between acoustic perturbations and the vorticity field is strong [5]. Function of the frequency, the interaction dissipates or creates an amount of acoustic power [2]. Self-sustained oscillations can thus be created when a resonant acoustic field at a frequency in the amplification range exists in the pipe [4]. This resonant field is a consequence of acoustic reflections at elements upstream and downstream of the orifice. The final whistling features are set by non-linear saturation effects.

The present paper discuss the whistling ability of an orifice as well as the whistling features in a resonant pipe for low Mach number flows. We will present how, in that case, tools based on incompressible flow assumption around the orifice are able to represent the phenomena acting in whistling generation.

First, the whistling ability of an orifice will be estimated from incompressible flow simulations. The proposed methodology is based on the Unsteady Reynolds Averaged Navier-Stokes Equations (URANS) for an incompressible fluid and has been previously used by Martinez *et al.* [6] for a T junction between three pipes and by Nakiboğlu *et al.* [7] for cavities in pipes. The acoustic impedance of the orifice is determined from these simulations, and the whistling ability of an orifice is extracted. A good agreement is found with experimental data.

Then, we consider an orifice in a reverberating pipe. Considering the whole system composed of a nonlinear acoustic gain at the orifice and a linear acoustic feedback surrounding it, we analyse the evolution of the whistling frequency and amplitude obtained by previous experiments. We show that a linear stability analysis is able to predict the whistling frequency in such a configuration and how the whistling amplitude is related to the feedback term and to the Strouhal number.

2 Studied case

The case studied here corresponds to a circular orifice inserted in a pipe with upstream and downstream reflecting conditions. An air flow is present in the pipe. Figure 1 presents a scheme of the studied case.

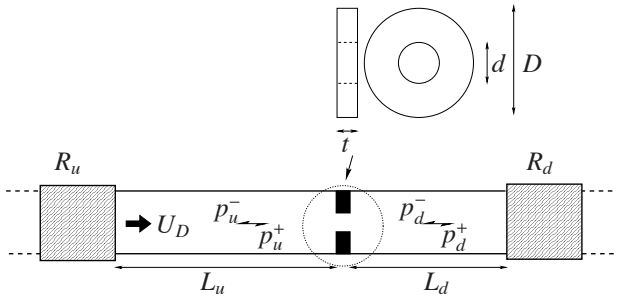

Figure 1: Scheme of the studied configuration

The main pipe diameter is $D = 0.03$ m. The orifice has a thickness $t = 0.005$ m and a diameter $d = 0.015$ m. Different main flow velocities U_D are tested in the range 6 to 12 ms^{-1}. These correspond to a Mach number M_D ranging from 0.017 to 0.035 and to a Reynolds number between 12000 and 24000.

3 Theoretical background

This section introduces the different phenomena responsible of pure tone noise generation by an orifice in confined flow. It only focuses on low Mach number such that the fluid compressibility inside the orifice does not play a significant role [8, 9]. In that case, as described in subsection 3.1, the acoustic dissipation at the orifice is totally defined by a single complex term, which can be the impedance or a equivalent gain expression. Then the surrounding reflection plays the role of a feedback mechanism. The stability can be treated by a linear stability analysis, the resulting whistling frequency and amplitude being determined by nonlinear saturation effect. These last free phenomena are treated respectively in subsections 3.2, 3.3 and 3.4.

3.1 Source model and impedance representation

For an incompressible fluid with a sufficiently high Reynolds number, in order to neglect the viscosity, and for harmonic perturbations of the background velocity, the pressure difference across the orifice can be expressed as [5, 8, 10]

$$\Delta P = (\rho c Z_s - j\rho\omega L_{ori})\, u'_z, \tag{1}$$

where ρ is the fluid density, c the speed of sound, $\omega/(2\pi)$ the frequency of the preturbation and u'_z the velocity perturbation. The first term of the equation defines the pressure

difference due to the vorticity field in the orifice jet and introduces the real part of impedance Z_s. It characterises all the dissipative acoustic effect of the orifice. The second term of the equation stands for the pressure difference created by a pureley potential flow accross the orifice. Both terms can be summarized in a complex impedance term $Z = Z_s - j\omega L_{ori}/c$.

The definition of the aeroacoustic feature of an orifice from an incompressible simulation needs so the determination of the complex impedance Z. The real part of the impedance characterizing the acoustic source is used to define the whistling ability of the orifice. Indeed, a negative value of the real part of the impedance term corresponds to a potential amplification of the incident acoustic fluctuation and so to a potential whistling case. The imaginary part of the impedance defines the inertial flow effect in the orifice. In this paper, Both of them are retrieving from an incompressible flow simulation as described in section 4.

Another representation of the acoustic dissipation due to the orifice submitted to flow can be used [4]. It corresponds to a gain representation and is very useful to take into account the surrounding reflection around the orifice. It takes the form

$$\begin{pmatrix} p_d^+ + p_u^- \\ p_d^+ - p_u^- \end{pmatrix} = \begin{pmatrix} 1 & 0 \\ 0 & \mathcal{G} \end{pmatrix} \begin{pmatrix} p_u^+ + p_d^- \\ p_u^+ - p_d^- \end{pmatrix}, \tag{2}$$

with $\mathcal{G} = (2 - Z)/(2 + Z)$ an acoustic gain. Acoustic amplification due to the flow trough the orifice can occur if the modulus of $\mathcal{G}$ is greater than one.

3.2 Acoustic reflection and feedback

Following the formalism of Eq. (2), the acoustic feedback of the surrounding pipe can be described by the equation

$$p_u^+ - p_d^- = \mathcal{F}\left(p_d^+ - p_u^-\right) \tag{3}$$

where $\mathcal{F}$ is a complex term defining the overall surrounding acoustic reflection. It corresponds to a reflection coefficient between the waves combinations $p_u^+ - p_d^-$ and $p_d^+ - p_u^-$ and takes the form

$$\mathcal{F} = \frac{R_u + R_d - 2R_uR_d}{R_u + R_d - 2}. \tag{4}$$

. The reflection coefficients in Eq. (4) correspond to the measured reflection coefficient translated at the orifice location

$$R_u = R_u^m \mathrm{e}^{-j(k^+ + k^-)L_u}, \tag{5}$$

and

$$R_d = R_d^m \mathrm{e}^{-j(k^+ + k^-)L_d}, \tag{6}$$

where L_u and L_d are the pipe lengths from the orifice to the upstream and to the downstream boundaries, respectively.

3.3 Linear stability analysis

The stability of the linear system composed of Eqs. (2) and (3) can be estimated with classical linear stability analysis [11, 12]. In that case, the important parameter is the product $\mathcal{GF}$, an instability of the system being predicted if this product is purely real and greater than one. This analysis performed in the linear regime allows to determine the stability of the system as well as the unstable frequencies. Unstable frequency and whistling frequency are compared in subsection 5.2. It lust be reminded that these two frequencies are different, the whistling frequency resulting from nonlinear saturation.

3.4 Acoustic balance in whistling regime

In steady whistling regime, it is assumed that the analysis can be focused on the fundamental frequency by introducing an equivalent acoustic gain. Doing so, the nonlinear nature of acoustic amplification, and the role played by harmonics of the fundamental frequency are neglected. The harmonic pressure peaks measured being lower by at least one order of magnitude than the fundamental peak, the nonlinear gain representation is assumed to hold without further proof. Let then the steady state regime be associated to a saturated value $\mathcal{G}_{sat}$ of the acoustic gain, according to

$$\begin{pmatrix} p_d^+ + p_u^- \\ p_d^+ - p_u^- \end{pmatrix} = \begin{pmatrix} 1 & 0 \\ 0 & \mathcal{G}_{sat} \end{pmatrix} \begin{pmatrix} p_u^+ + p_d^- \\ p_u^+ - p_d^- \end{pmatrix}. \tag{7}$$

This situation occurs whenever nonlinear effects inside the orifice adapt the acoustic gain to the acoustic feedback of the surrounding pipe. In other words, the steady state gain cannot be considered any longer as an intrinsic property of the orifice, it depends on the amplitude of the whistling.

Combining Eqs. (7) and (3), the balance of acoustic amplification and feedback can be written

$$\mathcal{G}_{sat}\mathcal{F} = 1. \tag{8}$$

The balance of gain and feedback described by Eq. (8) has the classical form of linear oscillator studies with a single degree of freedom [13]. The feedback term $\mathcal{F}$ is known to be a key parameter for the onset of self-sustained oscillations. In subsection 5.3, its value will be compared to whistling amplitudes.

4 Impedance characterization from incompressible flow simulation

In the present section, we focus on the determination of the impedance term defined in subsection 3.1. The determination of it is based on an incompressible flow simulation coupled with a source processing.

4.1 Description of the simulation

The simulation of an incompressible flow through an orifice is here achieved with solving the Unsteady Reynolds Averaged Navier-Stokes Equation (URANS). The numerical tools used in that way is *Code_Saturne* developed at EDF [14]. The turbulence model is the model $k - \omega$ SST [15].

The simulation is performed assuming an axisymmetric flow. The simulation is thus done on a radial section of the pipe. The computational domain begins at a distance $L_1 = 2.5D$ of the orifice and ends at $L_2 = 7D$ after the orifice.

The wall conditions correspond to the no-slip ones and a scalable wall law is used [14]. The mass flow rate is defined at the inlet. The velocity profile is chosen uniform here. The outlet corresponds to a Neumann's condition and set the pressure gradient across the outlet to zero.

The mesh of the domain is made of 99000 cells defined as cubic as possible. The refinement is maximum at the upstream edge of the orifice. This point corresponds to the beginning of the shear layer in the flow and its definition is crucial in the study of whistling generation. So in this area, the spatial discretization step is $\Delta r = \Delta z = 5 \times 10^{-5}$ m, with

r the radial direction and z the longitudinal direction. Expressed in wall units, based on a turbulent velocity profile with a mean velocity corresponding to the one in the orifice $U_d = U(D/d)^2$, this discretization step is $r^+ = z^+ \approx 5$. Far away from the orifice, the discretization is decreased up to a value $D/\Delta r = D/\Delta z \approx 45$.

The first step of the simulation consists of computing the mean flow solution. This is achieved after a physical time on order of 0, 03 s.

From the mean flow field solution, a fluctuating velocity $u'(t)$ is added at the inlet. This perturbation is uniform along the radius of the pipe. It has been chosen harmonic with a frequency f_{exc} and an amplitude A. It can thus be written

$$u'(t) = A\cos(2\pi f_{exc} t). \tag{9}$$

The amplitude of the excitations is chosen low enough to ensure a linear response of the orifice. Previous experimental studies [2] have shown that non linear effects appear for an amplitude of the excitations around few percent of the mean flow velocity. In the present case, the value is set to $A = 0.001U$. The excitation frequency f_{exc} takes values from 500 to 4000 Hz. The frequency step is equal to 200 Hz and is decreased down to 100 Hz in the amplification frequency range. For each frequency, the simulation time corresponds to four periods of the excitation signals. This value is sufficient for the convergence of the solution.

Using time pressure data stored at difference location along the pipes, the impedance term is identified from the signals of the excitation velocity and the pressure difference. The procedure of extraction is described in [7, 3, 10].

4.2 Results

The studied case has been characterized experimentally by Testud *et al.* [2]. It corresponds to the dimensions given in section 2. The flow velocity in the main pipe is $U_D = 9\ \mathrm{m{\cdot}s^{-1}}$. The Mach number is thus $M_D = 0.026$ and the Reynolds number $Re_D \approx 18000$. The studied frequency range extends from 500 to 4000 Hz.

The figures 2 and 3 present the real and imaginary parts of the impedance term Z. Experimental[1] and numerical results are compared.

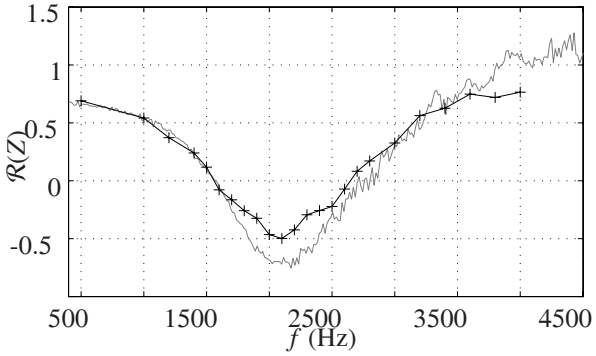

Figure 2: Real part of the impedance Z. Black line and cross: simulation, gray line: experiment.

In general a good agreement between experiments and numerics is observed on the real and imaginary plots. In the following, a description of each part of the impedance is done and the numerical and experimental results are compared.

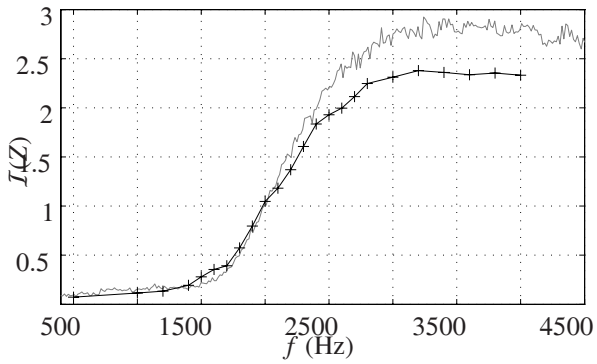

Figure 3: Imaginary part of the impedance Z. Black line and cross: simulation, gray line: experiment.

First, the real part of the impedance Z plotted in figure 2 is studied. It characterizes the acoustic dissipation at the orifice and is thus used to study the acoustic ability of an orifice. Before 1500 Hz, the real part of Z is positive. In the corresponding frequency range, only dissipation effects occur. In this range, a very good agreement is found between the experiments and the simulation. Then, between 1500 and 2700 Hz, the real part of Z becomes negative. This corresponds to a frequency range where acoustic perturbations can be amplified. The presence of the orifice in the flow can thus create a whistling if the surrounding acoustic reflections are sufficiently high [4, 2]. This frequency range is predicted with the numerical procedure, but some discrepancies are observed compare to the experiments. These differences correspond in the numerical results to an overestimation of the real part of Z and a shift of the end of the amplification range toward the low frequencies. Finally, beyond 2700 Hz, the real part of Z becomes positive again and only acoustic dissipation occurs. In this frequency range up to 3700 Hz, experiments and numerics are in good agreement. Slight differences appear above 3700 Hz.

Then, the imaginary part of the impedance Z is studied. It characterizes the inertial effects in the orifice. Below 1500 Hz, the imaginary part of Z increases very slowly. As for the real part the agreement is good between experiments and simulation. Between 1500 and 2700 Hz, corresponding to the potential whistling frequency range, the slope of the imaginary part of Z is sharp and almost constant. In this frequency range, a good agreement between the experimental and numerical results is observed up to 2000 Hz. Beyond this value discrepancies are observed, which becomes larger as the frequency is closer to the limit of the range 2700 Hz. In this frequency range, differences have also been observed in the real part of Z, and as the high frequency limit of the amplification range is underestimated in the real part, the difference observed in the imaginary part may have the same origin. Finally beyond 2700 Hz, the imaginary part becomes almost constant as well in the experiments and in the numerics. The values are however different but it may be a consequence of the differences observed earlier in frequency.

Even if some discrepancies have been observed, the numerical procedure gives promising results and an incompressible URANS simulation is able to predict accurately the potential whistling frequency range of an orifice. More generally, the aeroacoustical behavior of an orifice over a broad

[1] In the experiments, the scattering matrix of the orifice has been measured. Considering the incompressible flow assumption, it is easy to express the impedance term as function of the scattering matrix coefficients [3, 10].

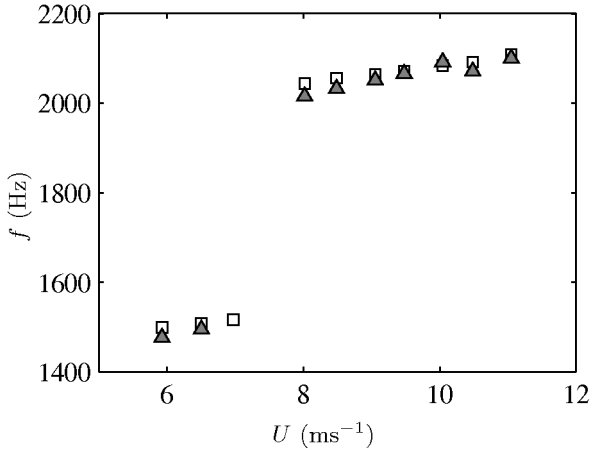

Figure 4: Comparison between the calculated unstable frequencies (gray triangles) and the measured whistling frequencies (white squares).

frequency range has been predicted with the simulation.

5 Characterization of whistling frequency and amplitude

After studying the acoustic amplification at the orifice, we focus on characterizing the whistling frequency and amplitude when an orifice is surrounded by acoustic reflection conditions. Experiments have been previously performed [4, 3]. They are used here to compare the whistling frequencies to the unstable frequencies obtained with the linear stability analysis. Also, the experimental data are used to show the parameters controlling the whistling amplitude.

5.1 Description of the experiments

The description of the experiments is well detailed in [4, 3]. Be it enough here to mention that we use experiments being made with a constant upstream high reflecting condition and three different downstream condition having a decreasing reflection coefficient modulus. The pipe and the orifice have the dimensions given in section 2. For each of the three configurations, the flow velocity ranges from 6 to 12 ms^{-1}.

During the experiments, the whistling frequencies and amplitude are measured. Also, the reflection coefficient of the upstream and the three downstream boundary conditions are known. They are used to calculate the feedback term $\mathcal{F}$. The acoustic gain $\mathcal{G}$ of the orifice is calculated from the orifice impedance obtained in subsection 4.2.

5.2 Whistling frequency and instability frequency

Figure 4 presents the evolution of the whistling frequency with the flow velocity for one of the three cases introduced in subsection 5.1. It is first observed that whistling frequencies are locked on successive acoustic modes, in a manner similar to unstable grazing flows above cavities [16, 5, 7].

In figure 4, two ranges of frequency around 1500 Hz and 2100 Hz are observed for velocities below and above 8 ms^{-1}, respectively. The frequency step is the signature of the shift from one acoustic mode to another when the flow velocity is increased. The whistling frequency corresponds to an acoustic mode of the orifice and of the surrounding pipe. Defining the Strouhal number $St = ft/U_{hole}$, with t the orifice thickness and U_{hole} the flow velocity in the orifice, the whistling frequencies lie in the range 0.2 — 0.4, consistent with the acoustic amplification range in figure 2. More precisely, the first acoustic mode in figure 4 is associated to a Strouhal number varying from 0.32 to 0.27, and the second acoustic mode is associated to a Strouhal number varying from 0.32 to 0.23. For each range of frequency, the full range of Strouhal numbers prone to whistling is covered as the flow velocity increases.

The gray triangles of figure 4 label the unstable frequencies derived from the linear stability analysis given in section 3.3. The unstable frequencies predicted by the linear analysis fairly agree with the measured whistling frequencies. For practical purposes, it can be assessed that self-sustained oscillations occur at a frequency such that the product $\mathcal{GF}$ is a real number, with a value higher than unity. Whistling can hence appear if the feedback term $\mathcal{F}$ has a modulus typically higher than 0.5, and if the frequency corresponds to a Strouhal number in the range 0.2 — 0.4.

Even if the unstable frequencies and the whistling frequencies are very close, it must be kept in mind that they are different as the whistling frequencies result from nonlinear saturation phenomenon, as described in subsection 3.4. The results obtained here show however that these two frequencies are very close so that further work is needed to study there differences.

5.3 Whistling amplitude

In this last subsection, we focus on the evolution of the whistling amplitude with the acoustic feedback term $\mathcal{F}$ and the Strouhal number. For this paper, we study only whistling occurring on a single acoustic mode, particularly the one around 2100 Hz in figure 4. As a reminding, three arrangements are studied, having similar phase conditions and having decreasing modulus of the downstream reflection condition. The modulus of this reflection coefficient varies from 0.5 to 0.8, so that the acoustic modes of the system are only slightly altered between each arrangement.

As presented in figure 5, the dimensionless acoustic velocity varies from 1% to about 15% and the amplitude of whistling is dependant on both the modulus of the acoustic feedback $\mathcal{F}$ and the Strouhal number. This amplitude increases with the feedback modulus (see figure 5b), and it exhibits a maximum for a Strouhal number of the order of 0.25 (see figure 5a). This value of 0.25 correspond to the value which makes the linear gain maximum, or the real part of the acoustic impedance minimum (see figure 2). Moreover, the comparison of the three curves of figure 5a indicates a variation of the Strouhal number associated to the maximum amplitude with the feedback modulus. This point needs more data to be investigated.

6 Conclusion

The present paper has shown how incompressible tools are able to capture the acoustical behavior of an orifice in the case of low Mach number.

First, using an URANS approach, incompressible simulations of a pipe flow impinging an orifice with superimposed

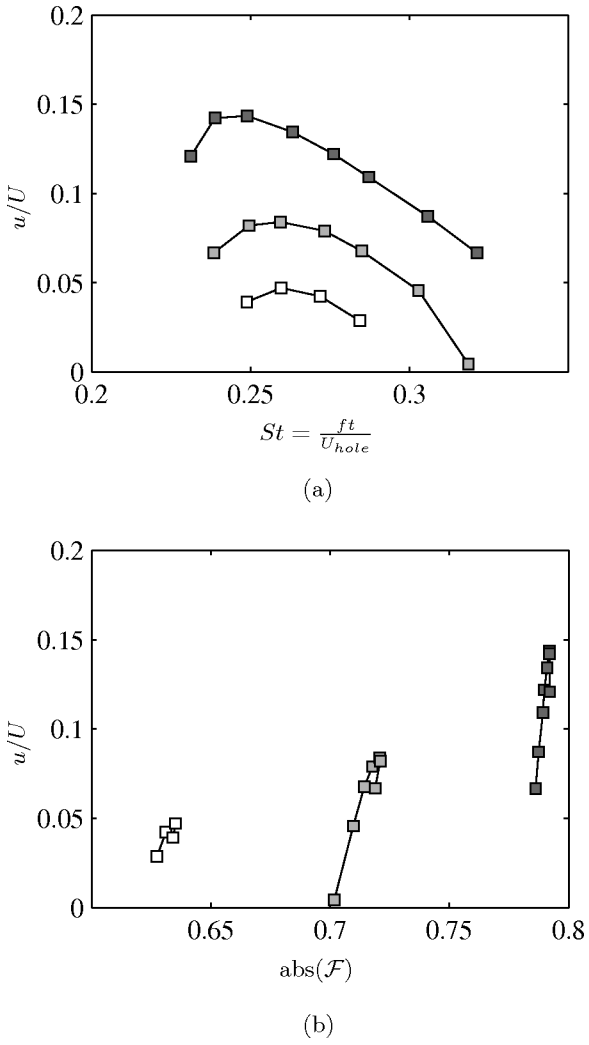

Figure 5: Evolution of the dimensionless whistling amplitude with the Strouhal number, (a), and with the modulus of $\mathcal{F}$, (b), for one single mode. The dark gray squares correspond to the case with the most reflecting downstream condition, the light gray to the intermediate one and the white squares to the less reflecting one.

harmonic velocity fluctuations have been used to extract an impedance term Z in the frequency range 500-4000 Hz. A comparison of this impedance to experimental results show a good agreement. From the real part of Z, it is moreover possible to define the whistling ability of an orifice and the method presented here predicted accurately the potential whistling frequency range.

Then, studying the whole system as a closed loop composed of an nonlinear acoustic gain and a linear acoustic feedback has allowed to characterize the evolution of the whistling frequency and amplitude. On one hand, a linear stability analysis predicts accurately the whistling frequency of the system. On the other hand, the analysis of whistling amplitude shows that the whistling amplitude increases with the acoustic feedback of the system and that it is maximum for a Strouhal number around 0.25.

References

[1] A B C Anderson. A jet-tone orifice number for orifices of small thickness-diameter ratio. *J. Acoust. Soc. Am.*, 26(1):21–25, 1954.

[2] P Testud, Y Aurégan, P Moussou, and A Hirschberg. The whistling potentiality of an orifice in a confined flow using an energetic criterion. *J. Sound Vib.*, 325(4):769–780, 2009.

[3] R Lacombe. *Sifflement de diaphragmes en conduit soumis à un écoulement subsonique turbulent*. PhD thesis, Université du Maine, Académie de Nantes, Le Mans, France, 2011.

[4] R Lacombe, P Moussou, and Y Aurégan. Whistling of an orifice in a reverberating flow duct. *J. Acoust. Soc. Am.*, 130(5):2662–2672, 2011.

[5] M S Howe. *Acoustic of œuid-structure interaction*. Cambridge University Press, 1998.

[6] P Martinez-Lera, C Schram, S Föller, R Kaess, and W Polifke. Identification of the aeroacoustic response of low Mach number flow through a T-joint. *J Acoust. Soc. Am.*, 162(2):582–586, 2009.

[7] G Nakiboğlu, S P C Belfroid, J Golliard, and A Hirschberg. On the whistling corrugated pipes: effect of pipe length and flow profile. *J. Fluid Mec.*, Soumis, 2011.

[8] G Hofmans, M Ranucci, G Ajello, Y Aurégan, and A Hirschberg. Aeroacoustic response of a slit-shaped diaphragm in a pipe at low Helmholtz number, 2: unsteady results. *J. Sound Vib.*, 244(1):37–77, 2001.

[9] P Moussou, P Testud, Y Aurégan, and A Hirschberg. An acoustic criterion for the whistling of orifices in pipes. In *ASME 2007 Pressure Vessels and Piping Conference*, 2007.

[10] R Lacombe, P Moussou, and Y Aurégan. Identification of whistling ability of a single hole orifice from incompressible flow simulation. In *ASME 2011 Pressure Vessels and Piping Conference*, 2011.

[11] T Sattelmayer and W Polifke. A novel method for the computation of the linear stability of combustors. *Combust. Sci. Tech.*, 175:477–497, 2003.

[12] M Karlsson and M Åbom. On the use of linear acoustic multiports to predict whistling in confined flows. *Acta Acustica united with Acustica*, 97:24–33, 2011.

[13] T D Mast and A D Pierce. Describing function theory for flow excitation of resonators. *J. Acoust. Soc. Am.*, 97(1):163–172, 1995.

[14] F Archambeau, N Méchitoua, and M Sakiz. *Code_Saturne*: a finite volume code for the computation of turbulent incompressible flows - industrial applications. *Int. J. Finite Volumes*, 1(1), 2004.

[15] F R Menter. Two-equations eddy-viscosity turbulence models for engineering applications. *AIAA Journal*, 32(8):1598–1605, 1994.

[16] D Rockwell and E Naudascher. Self-sustained oscillations of impinging free shear layers. *Annual Review of Fluid Mechanics*, 11:67–94, 1979.